



**Calhoun: The NPS Institutional Archive**  
**DSpace Repository**

---

Faculty and Researchers

Faculty and Researchers' Publications

---

2017

## Continuous-wave laser particle conditioning: thresholds and time scales

Brown, Andrew; Ogloza, Albert; Olson, Kyle; Talghader, Joseph  
Elsevier

---

A. Brown, A. Ogloza, K. Olson, J. Talghader, "Continuous-wave laser particle conditioning: thresholds and time scales," *Optics and Laser Technology*, v. 89 (2017), pp. 27-30.

<http://hdl.handle.net/10945/55403>

---

This publication is a work of the U.S. Government as defined in Title 17, United States Code, Section 101. Copyright protection is not available for this work in the United States.

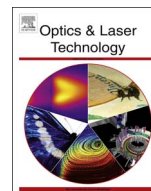
*Downloaded from NPS Archive: Calhoun*



Calhoun is the Naval Postgraduate School's public access digital repository for research materials and institutional publications created by the NPS community. Calhoun is named for Professor of Mathematics Guy K. Calhoun, NPS's first appointed -- and published -- scholarly author.

**Dudley Knox Library / Naval Postgraduate School**  
**411 Dyer Road / 1 University Circle**  
**Monterey, California USA 93943**

<http://www.nps.edu/library>



# Continuous-wave laser particle conditioning: Thresholds and time scales



Andrew Brown<sup>a</sup>, Albert Ogloza<sup>b</sup>, Kyle Olson<sup>a</sup>, Joseph Talghader<sup>a,\*</sup>

<sup>a</sup> Electrical Engineering, University of Minnesota, Minneapolis, MN 55455, USA

<sup>b</sup> Naval Postgraduate School, 1 University Cir, Monterey, CA 93943, United States

## ARTICLE INFO

### Keywords:

Laser damage  
Laser conditioning  
Continuous-wave

## ABSTRACT

The optical absorption of contaminants on high reflectivity mirrors was measured using photo thermal common-path interferometry before and after exposure to high power continuous-wave laser light. The contaminants were micron-sized graphite flakes on hafnia-silica distributed Bragg reflectors illuminated by a ytterbium-doped fiber laser. After one-second periods of exposure, the mirrors demonstrated reduced absorption for irradiances as low as  $11 \text{ kW cm}^{-2}$  and had an obvious threshold near  $20 \text{ kW cm}^{-2}$ . Final absorption values were reduced by up to 90% of their initial value for irradiances of  $92 \text{ kW cm}^{-2}$ . For shorter pulses at  $34 \text{ kW cm}^{-2}$ , a minimum exposure time required to begin absorption reduction was found between 100  $\mu\text{s}$  and 200  $\mu\text{s}$ , with particles reaching their final minimum absorption value within 300 ms. Microscope images of the surface showed agglomerated particles fragmenting with some being removed completely, probably by evaporation for exposures between 200  $\mu\text{s}$  to 10 ms. Exposures of 100 ms and longer left behind a thin semi-transparent residue, covering much of the conditioned area. An order of magnitude estimate of the time necessary to begin altering the surface contaminants (also known as "conditioning") indicates about 200  $\mu\text{s}$  seconds at  $34 \text{ kW cm}^{-2}$ , based on heating an average carbon particle to its sublimation temperature including energy loss to thermal contact and radiation. This estimation is close to the observed exposure time required to begin absorption reduction.

## 1. Introduction

Increasingly powerful CW laser systems are demanding low absorption, high damage threshold optics for beam control. While these optics, when pristine, can operate at irradiances of multiple  $\text{MW cm}^{-2}$ , particle contamination can drastically reduce their damage thresholds [1,2]. Careful contamination control and regular cleaning are the preferred methods to alleviate these problems; however, many situations require operation even when faced with random contaminants.

Although the exposure of contaminated optics to high irradiances often leads to catastrophic failure, lower irradiance exposure can have a beneficial conditioning effect on the optic [3,4]. Optics that have been laser-conditioned experience less heating and survive higher irradiances than non-conditioned optics [5]. A CW laser system that could self-clean and condition with a low power initial start-up shot would be highly desirable. Pulsed lasers have long been studied and used for laser cleaning [6], though less research has been focused on continuous-wave laser cleaning.

To better understand the laser conditioning process, we must find the irradiance and duration of exposure required to cause a reduction in absorption. With these values known, we can model the physical

processes at work in conditioning and determine the feasibility of using such conditioning as a means of preventing laser damage.

## 2. Optics and contamination

High reflectivity hafnia-silica distributed Bragg reflectors (DBR's) were contaminated with a suspension of graphite particles in isopropyl alcohol and then gently blown dry using compressed air. The graphite particles were  $1 \mu\text{m}$  natural graphite flakes from SkySpring Nanomaterials. Graphite was chosen as previous testing found it to be particularly harmful to optical coatings [5]. The size and shape of the particles were measured using optical and electron microscopes. Individual particles were close to  $1 \mu\text{m}$  in size though they formed agglomerates varying substantially from volumes of  $1 \mu\text{m}$  on a side to over  $10 \mu\text{m}$  on a side. Half the agglomerates were larger than  $4 \mu\text{m}$  in at least one dimension with 10% being larger than  $7.5 \mu\text{m}$ .

The DBRs used for testing were optimized for maximum reflectivity at 1064 nm and consisted of 89 layers of hafnia and silica, the top and bottom layers being silica. Absorption without particle contamination was measured at 7 ppm and less. With the graphite contamination absorption values increased to 1000–10,000 ppm. The damage thresh-

\* Corresponding author.

E-mail address: [joey@umn.edu](mailto:joey@umn.edu) (J. Talghader).

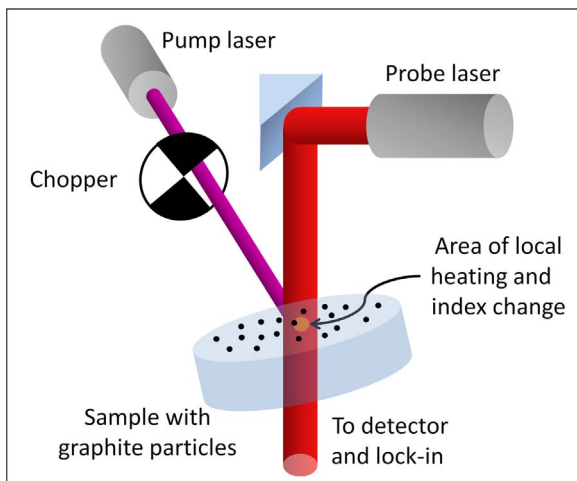


Fig. 1. Conceptual diagram of a photothermal common-path interferometry system.

old of the DBRs was over  $13 \text{ MW cm}^{-2}$  before contamination. After contamination laser induced damage occurred between  $1\text{--}3 \text{ MW cm}^{-2}$ . The substrate underlying the DBR coating was  $6.35 \text{ mm}$  of fused silica.

### 3. Absorption measurement and sample testing

The initial optical absorption at  $1064 \text{ nm}$  of the graphite particles and coated optic was measured using a photo thermal common-path interferometry (PCI) system from Stanford Photo-Thermal Solutions. A  $10 \text{ W}$   $1064 \text{ nm}$  Ytterbium-doped fiber laser was used as the pump source for the PCI system.

PCI measures the optical absorption of a sample by periodically heating a local region using a chopped pump laser at the wavelength of interest, see Fig. 1. The  $dn/dt$  of the sample creates a phase change that affects a small portion of the HeNe probe laser. The local phase change causes self interference of the probe beam, creating an amplitude difference that is measured via a lock-in amplifier at the frequency of the chopped pump beam [7].

A large pump laser spot size of  $110 \mu\text{m}$  was used during the PCI measurement to capture the absorption of multiple graphite particles at each sample location measured, increasing the total number of particles surveyed. A low pump power of  $320 \text{ mW}$ , yielding an average irradiance  $3.4 \text{ kW cm}^{-2}$ , was used to prevent unintentional particle heating and conditioning during measurement. Locations tested were spaced apart by  $300 \mu\text{m}$  to prevent any cross effects from neighboring locations.

After the initial absorption measurement, the chopper wheel was removed and the pump laser power momentarily increased to condition the location. The time of exposure was controlled with a function generator used to drive the fiber laser, and the optical output was measured with a photodiode to ensure accurate timing. After laser conditioning, the pump power was reduced back to its measurement value, and the chopper wheel was replaced. A second absorption measurement was conducted and the fractional absorption reduction was recorded.

To find the conditioning threshold of particles under steady state conditions, long  $1 \text{ s}$  exposures were tested at different irradiances. Once a clear threshold was determined, shorter exposure times were tested at an irradiance above the long duration threshold to test for effects relating to the exposure time.

### 4. Results

Long  $1 \text{ s}$  laser exposures caused a reduction in absorption for irradiances of  $11 \text{ kW cm}^{-2}$  and higher, see Fig. 2. Significant absorption occurred beginning at an obvious threshold near  $20 \text{ kW cm}^{-2}$ .

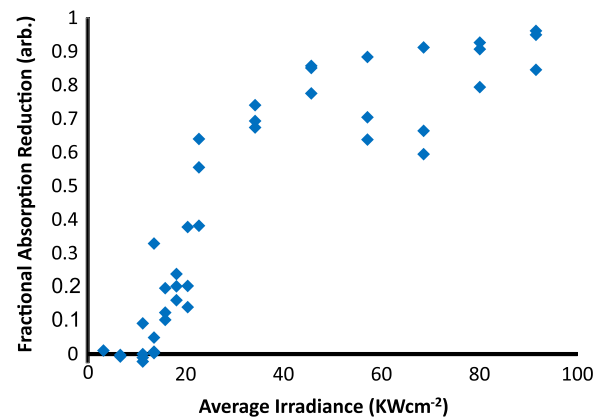


Fig. 2. Particle absorption reduction vs. irradiance for  $1 \text{ s}$  laser exposure. Note the threshold irradiance near  $20 \text{ kW cm}^{-2}$  required for significant absorption change.

Higher irradiances were found to cause greater sample conditioning with final absorption values after laser exposure being reduced by upwards of  $90\%$  of their original values.

Tests conducted at  $34 \text{ kW cm}^{-2}$  for shorter time exposures revealed a minimum exposure time of  $100 \mu\text{s}$  was required for any absorption change to occur, at least at the power levels available to our system, see Fig. 3. Absorption changes from  $100 \mu\text{s}$  to  $100 \text{ ms}$  were varied, though trended towards greater absorption reduction and more thorough conditioning for longer exposures. The final absorption values at  $300 \text{ ms}$  and  $1 \text{ s}$  closely matched near  $75\%$  absorption reduction, indicating that the extra  $700 \text{ ms}$  of exposure in the  $1 \text{ s}$  tests did little to further the conditioning process. Effectively all meaningful conditioning occurred within  $300 \text{ ms}$  and further exposure did not decrease absorption.

Optical microscope images of the  $34 \text{ kW cm}^{-2}$  conditioned areas showed that many particles were fragmented, with some being completely removed, see Fig. 4. Small areas of translucent, reddish halos are seen to appear around some particles. Longer exposures more thoroughly removed particles within the beam spot and areas covered by the reddish residue became quite large, covering an area equal to or greater than that of the original particles. Scanning electron microscope (SEM) images confirmed that the reddish hue is a flat residue on the surface of the substrate, see Fig. 5. The residue is mechanically affixed to the surface, and could not be removed by drag wipe cleaning. Earlier composition studies of such residue using time of flight secondary ion mass spectroscopy (TOF-SIMS) found the residue to be high in hydrocarbon species [5]. Images taken before  $100 \mu\text{s}$  show no visible particle changes, and images taken at  $300 \text{ ms}$  and  $1 \text{ s}$  are virtually identical regarding the extent of conditioning. This agrees with the PCI data of Fig. 3, indicating the minimum exposures required

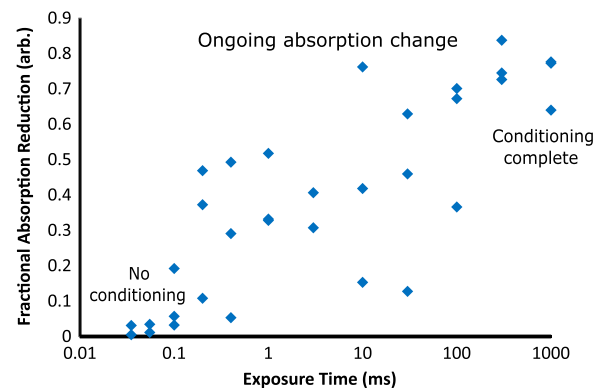
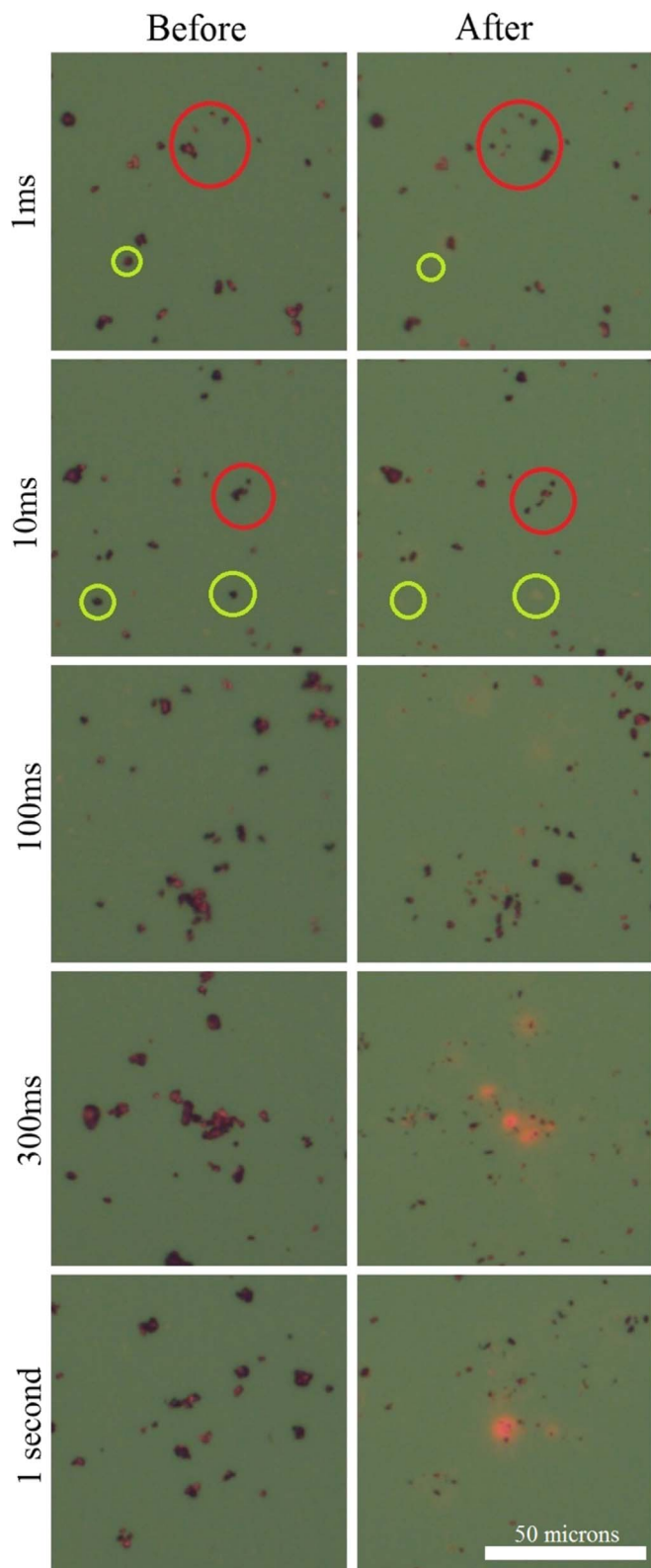
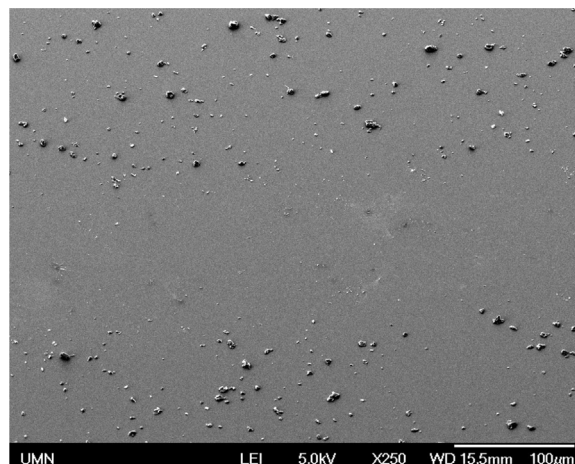


Fig. 3. Particle absorption reduction vs. exposure time for  $34 \text{ kW cm}^{-2}$  irradiance. Note that the first absorption change occurs around  $100 \mu\text{s}$ , and the final absorption values are reached by  $300 \text{ ms}$ .



**Fig. 4.** Particles before (left) and after (right) laser exposure at  $34 \text{ kWcm}^{-2}$ . Particles are seen to fragment (red circles) and be removed (green circles). Faint reddish halos are seen around some particles, indicating a local surface change. Longer exposures more thoroughly remove particles, and the presence of a conditioned residue becomes obvious by 300 ms.

to begin and finalize conditioning.



**Fig. 5.** SEM image of particle removal. The flat residue left behind after laser conditioning is seen in the middle third of the image. The image was taken at  $40^\circ$  to highlight topography differences.

## 5. Discussion

In order to better understand the laser conditioning process, it is useful to compare the measured conditioning timescales with those estimated from the physical properties of the particles. While calculating the energies entering the particles from laser irradiation and leaving from thermal radiation are relatively straightforward, estimating the thermal loss due to contact with the substrate is more uncertain. At the threshold of conditioning, we assume the particle temperature is just high enough to reach the sublimation temperature of carbon, 4000 K [8]. Given steady state conditions, the power entering and leaving the particle at this temperature and irradiance are the same, allowing us to estimate the contact conductance with the substrate, see Eq. (1).

$$H_i = \frac{A_{abs} * I_T - A_{emit} * \sigma * T_c^4}{T_c - T_s} \quad (1)$$

Where  $H_i$  is the contact conductance,  $I_T$  the threshold irradiance,  $A_{abs}$  is the particle cross-sectional area absorbing incident light,  $A_{emit}$  is the particle area emitting thermal radiation,  $T_c$  the temperature required to condition,  $T_s$  is the substrate temperature, and  $\sigma$  is the Stefan-Boltzmann constant. Note that the contaminants are assumed to be perfect blackbodies. Using a  $10 \mu\text{m}$  hemisphere for the model particle, the contact conductance is estimated at  $46 \text{ kWm}^{-2} \text{ K}^{-1}$ . This value initially seems high in comparison to metal-metal contacts which have a conductance on the order of a few  $\text{kWm}^{-2} \text{ K}^{-1}$  [9], however the contact conductance of graphene and highly ordered graphite can easily be tens of  $\text{MWm}^{-2} \text{ K}^{-1}$  [10]. The loose bonding of the graphite with the surface of the optic and the agglomerated nature of the graphite flakes may explain the lower value calculated.

With this order-of-magnitude estimate, the temperature of a particle under irradiation can be roughly approximated. Simulating the heating of the model particle, the particle is estimated to reach its sublimation temperature within  $240 \mu\text{s}$  for an irradiance of  $34 \text{ kW cm}^{-2}$ , close to the  $100\text{--}200 \mu\text{s}$  that was experimentally measured as the minimum required exposure to cause absorption changes.

In order to completely condition the surface, far more exposure time was required. This additional exposure time is likely due to some particles thermally bonding to the substrate during the first part of exposure. With the particles and substrate bonded, the contact conductance is increased and a much larger effective mass must be heated in order to fully condition the area.

## 6. Summary

In summary, laser conditioning of contaminated surfaces shows an obvious minimum threshold intensity beyond which the surface absorption begins to decrease due to particle removal and fracturing. Photothermal common-path interferometry provides an effective means of characterizing the laser conditioning process as both a function of time and irradiance. For long duration exposures, a conditioning threshold irradiance of  $20 \text{ kW cm}^{-2}$  was found to be required to cause significant absorption reduction. With high enough irradiances, conditioning reduced absorption by over 90%. Shorter exposures were also found to have a minimum time required to begin particle conditioning and also a minimum time required to reach full conditioning. Images of particles taken at different times show fragmentation, particle removal, and residue creation.

Simulation results using a thermal contact conductance found from the long duration conditioning threshold indicate that several hundred microseconds of exposure at  $34 \text{ kW cm}^{-2}$  is enough to heat particles to the point of sublimation. This agrees with some of the absorption reduction and particle change observed. The exposure time to fully condition samples however is several hundred milliseconds at  $34 \text{ kW cm}^{-2}$ . The extra time required to fully condition is most likely due to the particles thermally bonding with the substrate. This is seen as a thin residue that covers much of the conditioned area. With the contamination and substrate in close thermal contact, more energy, and thus more exposure time is required to heat the thermal mass to the point of being fully conditioned.

## Funding

Joint Technology Office (JTO); Office of Naval Research (N00014-12-1-1030).

## Acknowledgments

The authors thank ATFilms for providing the high reflectivity optics tested. Characterization of samples and carbon particles took place

using the University of Minnesota Nanofabrication center, and at the University's Characterization Facility.

## References

- [1] J.R. Palmer, Continuous wave laser damage on optical components, *Opt. Eng.* 22 (4) (1983) 224435–224435, URL (<http://opticalengineering.spiedigitallibrary.org/article.aspx?articleid=1222508>).
- [2] R.S. Shah, J.J. Rey, A.F. Stewart, Limits of performance: CW laser damage, in: G.J. Exarhos, A.H. Guenther, K.L. Lewis, D. Ristau, M.J. Soileau, C.J. Stolz (Eds.), *Proceedings. SPIE* 6403, 2006, pp. 640305–640305-14. <http://dx.doi.org/10.1117/12.695918>. URL (<http://proceedings.spiedigitallibrary.org/proceeding.aspx?Articleid=1295058>).
- [3] H. Bercegol, What is laser conditioning: a review focused on dielectric multilayers, in: *Laser-Induced Damage in Optical Materials: 1998*, International Society for Optics and Photonics, 1999, pp. 421–426. URL (<http://proceedings.spiedigitallibrary.org/proceeding.aspx?Articleid=974464>).
- [4] M.R. Kozlowski, M.C. Staggs, F. Rainer, J.H. Stathis, Laser conditioning and electronic defects of HfO<sub>2</sub> and SiO<sub>2</sub> thin films, in: *Laser-Induced Damage in Optical Materials: 1990*, International Society for Optics and Photonics, 1991, pp. 269–282. URL (<http://proceedings.spiedigitallibrary.org/proceeding.aspx?Articleid=959852>).
- [5] A. Brown, A. Ogloza, L. Taylor, J. Thomas, J. Talghader, Continuous-wave laser damage and conditioning of particle contaminated optics, *Appl. Opt.* 54 (16) (2015) 5216. <http://dx.doi.org/10.1364/AO.54.005216> URL (<https://www.osapublishing.org/abstract.cfm?URI=ao-54-16-5216>).
- [6] A.C. Tam, W.P. Leung, W. Zapka, W. Ziemlich, Laser-cleaning techniques for removal of surface particulates, *J. Appl. Phys.* 71 (7) (1992) 3515. <http://dx.doi.org/10.1063/1.350906>.
- [7] A. Alexandrovski, M. Fejer, A. Markosian, R. Route, Photothermal common-path interferometry (PCI): new developments, in: W.A. Clarkson, N. Hodgson, R.K. Shori (Eds.), *Proceedings. SPIE* 7193, 2009, pp. 71930D–71930D-13. <http://dx.doi.org/10.1117/12.814813>. URL (<http://proceedings.spiedigitallibrary.org/proceeding.aspx?Articleid=1332677>).
- [8] J. Abrahamson, Graphite Sublimation Temperatures, Carbon Arcs and Crystalline Erosion, *Carbon* 12 (2) (1974) 119–141. [http://dx.doi.org/10.1016/0008-6223\(74\)90019-0](http://dx.doi.org/10.1016/0008-6223(74)90019-0) URL ([http://ac.els-cdn.com/0008622374900190/1-s2.0-0008622374900190-main.pdf?\\_tid=39dc4ae6-c5f2-11e5-8243-00000aacb361\[\[\]\]\(#38;acdnat=1454008164\\_69af906c438dd43a732fb2b42a07fec8\)](http://ac.els-cdn.com/0008622374900190/1-s2.0-0008622374900190-main.pdf?_tid=39dc4ae6-c5f2-11e5-8243-00000aacb361[[]](#38;acdnat=1454008164_69af906c438dd43a732fb2b42a07fec8))).
- [9] E. Wolff, D. Schneider, Prediction of thermal contact resistance between polished surfaces, *Int. J. Heat. Mass Transf.* 41 (22) (1998) 3469–3482. [http://dx.doi.org/10.1016/S0017-9310\(98\)00067-2](http://dx.doi.org/10.1016/S0017-9310(98)00067-2).
- [10] Z. Chen, W. Jang, W. Bao, C.N. Lau, C. Dames, Thermal contact resistance between graphene and silicon dioxide, *Appl. Phys. Lett.* 95 (16) (2009) 161910. <http://dx.doi.org/10.1063/1.3245315>.